Dust remobilization from rough planar surfaces in tokamak steady-state plasmas

A. Autricque, S. Peillon, F. Gensdarmes, Moustapha Sow, N. Fedorczak, H. Roche, O. Pluchery, C. Grisolia

Dust remobilization from rough planar surfaces in tokamak steady-state plasmas

A. Autricque[a], S. Peillon[b], F. Gensdarmes[b], M. Sow[b], N. Fedorczak[a], H. Roche[a], O. Pluchery[c], C. Grisolia[*,a,d]

[a] *CEA, IRFM, F-13108 Saint-Paul-Lez-Durance, France*
[b] *Institut de Radioprotection et de Sûreté Nucléaire (IRSN), Gif-sur-Yvette 91192, France*
[c] *Sorbonne Universités, UPMC-CNRS, Institut des Nanosciences de Paris, 4 place Jussieu 75252, Paris Cedex 05, France*
[d] *National Research Nuclear University "MEPhI", Moscow 115409 Russian Federation*

A B S T R A C T

The ability of tungsten (W) dust to be remobilized from rough tokamak plasma-facing surfaces is investigated in this study. Atomic Force Microscopy is used to evaluate the adhesion force distribution between W spheroids of $\sim 1-10$ μm radius and a rough W substrate. Our results confirm that the Rabinovich model describes reasonably well the mean adhesion force in tokamak-relevant surface roughness regimes. The external (electric and ion drag) forces are estimated as well using a simplified sheath model. The results reveal that micron-size dust can be resuspended by attainable electric fields in tokamak conditions.

1. Introduction

Dust sources could play an important role in the impurity balance of fusion plasmas [1]. A rigorous assessment of the forces acting on a dust grain adhered onto a planar surface is critical for the understanding of dust remobilization processes. Dust remobilization occurs when re-suspension forces exceed the adhesion force. Among the most common external forces encountered in tokamaks are electric forces due to the sheath potential drop, drag forces due to the collection and scattering of plasma particles and gravity, which can act either as part of the lifting force or add up to adhesion depending on the orientation of the surface. Dust remobilization in tokamaks has been extensively studied [2–6], but the adhesion forces were often neglected, leading to a significant underestimation of the resuspension threshold. This shortcoming is rightly pointed out in a recent work [7] where the adhesion forces from contact mechanics models Johnson-Kendall-Roberts (JKR) [8] and Derjaguin-Muller-Toporov (DMT) [9] are compared with typical values of external forces. Yet contact mechanics models are known to over-estimate the adhesion force by 2 to 3 orders of magnitude because they do not include the effects of surface roughness [10–12]. Moreover, the expression used for the ion drag force is not applicable since it does not account neither for the presence of the surface near the dust particle nor the sheath electric field. Finally, works mentioned above do not account for the fact that adhesion forces are log-normally distributed [10]. This means that dust remobilization is not a threshold process, but must be assessed in terms of resuspension probability. The adhesion force

between a dust particle and a surface can be measured by different techniques, such as: centrifugation [13–16], aerodynamic detachment [17–19], vibration [20], inertial detachment [21,22], or electrostatic detachment [23–26]. The latter has been recently used to assess the mean and spread of the log-normal distribution of adhesion forces for fusion-relevant materials on relatively smooth surfaces [27–29]. In accordance with the low surface roughness used in these measurements, the adhesion forces obtained were close to that of a spherical particle on a perfectly planar surface, given by the classical van der Waals expression [30], i.e., in the μN range for the particle sizes considered. Yet these values of surface roughness might not be representative of tokamak plasma-facing surfaces. The aim of this paper is to investigate dust remobilization from rough surfaces in tokamaks. Measurements of the mean and spread of adhesion forces on fusion-relevant samples are performed via Atomic Force Microscopy (AFM), which is a reliable way to confront measurements with adhesion force model outcomes [31,32]. These measurements will be compared with the Rabinovich adhesion force model, which takes into account the surface roughness in the formulation of the van der Waals force [33]. Then, we estimate the remobilization efficiency of sheath electric forces in steady-state tokamak plasmas, considering adhesion and surface roughness. The paper is organized as follows: in Section 2, AFM measurements of pull-off forces are presented and results are compared with the Rabinovich adhesion model in order to assess the importance of the surface roughness. An expression for the dependence of the spread of adhesion forces on the particle size is proposed. In Section 3,

---

the model for the external forces in tokamak conditions is presented in details. In Section 4 the dust resuspension probability is calculated.

2. Direct measurement of adhesion forces

2.1. Experimental setup

Adhesion force measurements are performed with a Multimode 8 (Bruker) AFM in PeakForce Quantitative Nano-Mechanical mode (PF-QNM) in environmental conditions. Dust particles are glued to AFM cantilevers and the spring constant is measured. An AFM topographic image with a minimum 10×10 μm size composed of a matrix of 128×128 points at a scanning rate of 0.1 Hz is obtained with a peakforce amplitude of 300 nm. The adhesion force distribution is extracted from the adhesion image and fitted with a log-normal distribution to determine the mean and the spread for each particle size. For better accuracy, three different regions of the substrate are scanned, thus giving three log-normal adhesion force distributions. The substrate used is a 5×5 mm W surface exposed to He plasmas using radio-frequence (RF) hollow cathode discharges [34]. It is noteworthy to mention that this plasma exposure procedure allows the substrate to reach high temperatures (1000°C) and increases significantly its surface roughness. The roughness parameters, root mean square (rms_i) and peak-to-peak distances λ_i are measured by AFM in ScanAsyst mode (Bruker) with standard ScanAsyst probes on an 50×50 μm (2048×2048 points) area. The results are summarized in Table 1. The mean roughness is 712 nm with a maximum peak-to-valley height of 6.1 μm. For comparison, the surface roughness of the WEST tokamak divertor [35] was measured by confocal microscopy [36,37] prior to their installation in the machine. The roughness profile, averaged over 12 plasma-facing units, ranges between 800 nm and 1 μm and is close to the value recorded for the substrate used to perform the adhesion force measurements ($rms = 712$ nm). On the other hand, polished W substrates used in [27–29] are significantly smoother (10 nm $\leq rms \leq 200$ nm), and thus cannot be representative of all the surface states encountered in a tokamak. The used particles are W spheres manufactured by Tekna Advanced Material and were produced using a RF plasma discharge technique [38]. Selected particles of radii 3.58, 4, 5.45, 7.5 and 10.45 μm are grafted on tip-less CP-FM cantilevers following the method detailed in [39]. The roughness at the surface of the largest particle used (10.45 μm) is measured by AFM in tapping mode, on an area of 1.5×1.5 μm, which is much larger than its contact area with the substrate. The rms roughness measured is about 1 nm, which is much lower than the roughness of the substrate. Thus, in the following, particles are considered to be perfectly smooth. More details on the materials and methods are available in [40].

2.2. Results and discussion

The mean and spread of the adhesion force distribution against the dust radius r_d are plotted in Fig. 1. In order to extrapolate to any dust size, fit functions are required. The mean is fitted using the Rabinovich model [33], which is based on the van der Waals force and incorporates the contribution of two surface roughness scales, characterized by their root mean square roughness rms_1 and rms_2 as well as the peak-to-peak distances λ_1 and λ_2. The total adhesion force is simply the sum of the contribution of the adhesion of the dust particle with the different roughness structures and the underlying plane and is given by

$$\langle F_a \rangle = \frac{A_H r_d}{6H_0^2} \left[\frac{1}{1 + 58 rms_2 r_d / \lambda_2^2} + \frac{1}{(1 + 58 rms_1 r_d / \lambda_1^2)(1 + 1.82 rms_2 / H_0)^2} \right. $$
$$\left. + \frac{H_0^2}{(1 + 1.82(rms_1 + rms_2))^2} \right], \tag{1}$$

where A_H is the Hamaker constant and H_0 is the distance of closest approach. For W on W, $A_H = 4.98 \times 10^{-19}$ J. [41] $H_0 = 0.36$ nm is

commonly used [42], and this value fits the experimental measurements nicely for glass surfaces [40]. In the case of W, we found that $H_0 = 0.56$ nm fits better with the measurements for wide ranges of surface roughness [40]. The spread of the adhesion force distribution, σ, is fitted using a function proposed by Biasi, $\sigma(D_d) = A[1 + BD_d^C]D_d$, where $D_d = 2r_d$ is the particle diameter. We find, with D_d expressed in μm and σ in nN,

$$\sigma(D_d) = 0.0001[1 + 5.0131 D_d^{0.1002}]D_d. \tag{2}$$

The error bars in Fig. 1 correspond to the standard deviation of the three measurements of mean and spread adhesion force performed for each particle size. The adhesion force is very low, ~ 10 nN, compared to the classical van der Waals expression that would give a value of ~ 1 μN. This is related to the high surface roughness of the W substrate used. Thus such dust should be remobilized by plasma-induced forces because of their low adhesion force. Finally, gravity, which ranges between ~ 0.1 pN and ~ 0.1 nN for W dust with $r_d \sim 1 - 10$ μm is negligible compared to the measured adhesion forces.

3. External forces in tokamak conditions

In tokamaks, during plasma operation, a dust particle adhered to a surface is subjected to the following two main external forces: an electric force due to the Debye sheath electric field and an ion drag force (which increases adhesion). Modelling the sheath is mandatory to estimate them.

3.1. Sheath model

Here we use the simple sheath model from [3], where the plasma electron density n_e follows a Boltzmann law and the ions n_i are mono-kinetic combined with the flux conservation

$$n_e = n \times \exp\left(\frac{e\phi}{T}\right) \quad \text{and} \quad n_i = n\left[1 - 2\frac{e\phi}{T}\right]^{-1/2}, \tag{3}$$

where n and T are the plasma background density and temperature, respectively, ϕ denotes the plasma potential and e is the elementary charge. We assume singly charged ions and, at the sheath edge, quasi-neutrality, $T_e = T_i = T$, and an ion Mach number equal to 1. To express the electric field and the ion fluid velocity at the surface, the Poisson equation is integrated once, assuming zero potential and electric field at the sheath edge. We find

$$E = -\frac{T}{e\lambda_D}[2(e^{\varphi_w} + \sqrt{1 - 2\varphi_w} - 2)]^{1/2} \quad \text{and} \quad v_i = v_{\text{thi}}\sqrt{1 - 2\varphi_w}, \tag{4}$$

where φ_w is the wall potential normalized to T/e, $\lambda_D = \sqrt{\epsilon_0 T/(e^2 n)}$ is the Debye length, $v_{\text{thi}} = \sqrt{T/m_i}$ is the ion thermal velocity and m_i is the ion mass. φ_w is obtained by equating the electron and ion fluxes to the wall: $\varphi_w = \ln(2\pi m_e/m_i)/2$, where m_e is the electron mass. For deuterium ions, $\varphi_w \approx -3.19$. E is usually of the order of ~ 10 kV/cm. The typical thickness of the sheath is about $10\lambda_D$. In the following, we neglect the component of the ion flow that is parallel to the surface, which may induce rolling and sliding of the dust, to consider only the perpendicular component. Indeed, in tokamak plasmas, the magnetic field makes a grazing angle of $\approx 3°$ with the wall surfaces in order to protect the plasma-facing surfaces by reducing the perpendicular heat fluxes. Ions reaching the surface are initially following the magnetic field lines with a Larmor motion, making their initial parallel and perpendicular (to the surface) velocities hard to determine. Moreover, while flowing through the sheath, their potential energy is converted into more perpendicular velocity. In the following, the ion velocity is supposed to be oriented perfectly perpendicularly to the surface. This will result in an overestimation of the ion drag force on the dust grain, meaning that the remobilization probabilities determined in Section 4 are actually lower boundaries.
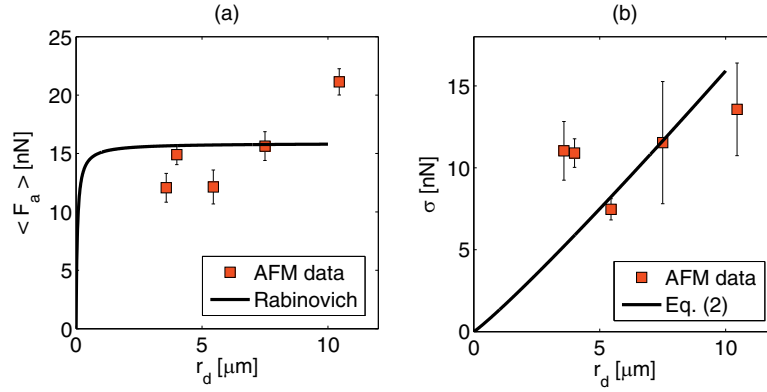
Fig. 1. Mean (a) and spread (b) of the adhesion force distribution, measured by AFM against the dust radius (squares). The force given by the Rabinovich model using the parameters in Table 1 and the fit for the spread are also plotted (lines).

Table 1
Surface roughness parameters, measured by AFM on the W substrate.

λ_1 (μm)	rms$_1$ (nm)	λ_2 (μm)	rms$_2$ (nm)
2.13	717	0.3	27

3.2. External forces

a. Dust electric charge Since intrinsic tokamak dust are exposed to little oxygen during and in between plasma discharges, the presence of any insulating oxide layer is neglected in the following. This allows the use of the expression of the electric charge of a conducting sphere laying on a conducting surface [43]

$$Q_d = \frac{2\pi^3}{3} r_d^2 \epsilon_0 E. \tag{5}$$

Q_d is typically of the order of a few thousand electric charges.

b. Electric force For a conducting particle laying onto a conducting substrate, the electric force applied on the grain is the combination of the Coulomb and image forces. The derivation of the image force is rather complex [43], but yields a simple expression when the particle and surface are in very close contact and the fluid in which the system is plunged is a perfect insulator. The total electric force is

$$F_e = \kappa 4\pi\epsilon_0 r_d^2 E^2, \tag{6}$$

where $\kappa = \zeta(3) + 1/6 \approx 1.37$, $\zeta(\cdot)$ is the Riemann zeta function [44]. Eq. (6) is often called the Lebedev formula. One could argue that the formation of oxide layers on the particles, due to the presence of oxygen in the vacuum vessel (when, for example, the machine is opened for maintenance), could challenge this ideal view. The electric force on a dielectric particle laying on a planar surface is the sum of the image, Coulomb and multipolar dielectrophoretic forces [43]

$$F_e = -\alpha \frac{Q_d^2}{16\pi\epsilon_0 r_d^2} + \beta Q_d E - \gamma 4\pi r_d^2 \epsilon_0 E^2, \tag{7}$$

where, in our case,

$$\alpha \approx 1, \quad \beta = 1 + \frac{1}{2}\delta, \quad \gamma = \frac{3}{8}\delta^2, \tag{8}$$

with $\delta = (\epsilon_d - 1)/(\epsilon_d + 2)$, ϵ_d being the particle dielectric constant. For a spherical particle composed of two materials of different dielectric properties, the equivalent dielectric constant ranges between the ones of the two materials and can be estimated using expressions presented in [43]. Eq. (7) is accurate at about 20%. The expression of the saturation charge of a spherical dielectric particle is used [45]

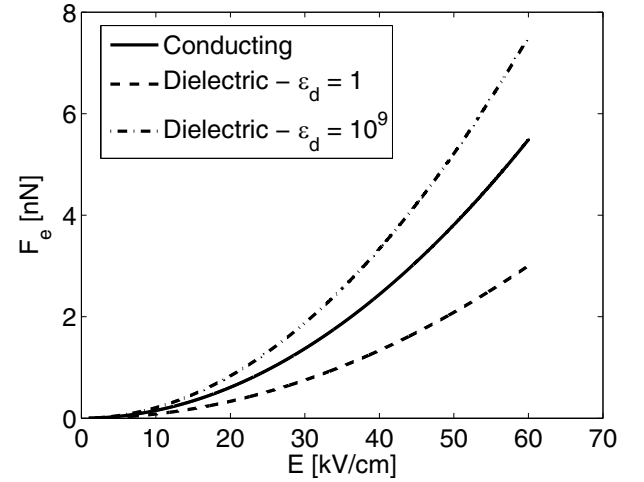$$Q_d = 12\pi\epsilon_0 \frac{\epsilon_d}{\epsilon_d + 2} r_d^2 E. \tag{9}$$

Fig. 2. Electric force against the electric field for a 1 μm conducting, Eq. (6), or dielectric, Eq. (7), particle. In the dielectric case, ϵ_d varies between 1 and 10^9.

The comparison between the electric forces on a dielectric and conducting particle of radius 1 μm is shown on Fig. 2. For the dielectric case, we varied ϵ_d between 1 and 10^9, given that (i) the value for W oxide (WO$_3$) is not well known in the literature and can be found to be 30 or above [46] and (ii) the thickness of the oxide layer affects the value of the dust equivalent dielectric constant. It is worth mentioning that Eq. (7) does not collapse to Eq. (6) for a conducting sphere ($\epsilon_d \gg 1$), owing to its approximate nature and because of the dust charge expression used, Eq. (9), which might not be perfectly accurate for a particle laying on a surface. Nevertheless, the difference between the two remains rather small, especially when compared to the wide variations of adhesion forces with the surface roughness. Thus the dielectric behavior of particles is not critical to the quantification of the electric force, even though it could play an important role on the adhesion force, through lower Hamaker constants. In this light, we choose to focus on the conducting case in the following.

c. Ion drag force In tokamak conditions, the other main actor impacting dust remobilization is the ion drag force. Since ions are accelerated from the sheath edge towards the wall, this force adds up to adhesion. When computed for an isolated dust grain immersed in a plasma, it is divided into the contributions from ions collected and scattered by the dust grain. Yet, in our case, the dust is located on a surface and scattered ions will transfer their momentum to the surface after little scattering by the grain, thereby making the contribution of collected ions the only significant one to the drag force. The ion drag force depends on the collection cross-section of the dust grain. In [7], the classical expression for isolated dust grains in Maxwellian-
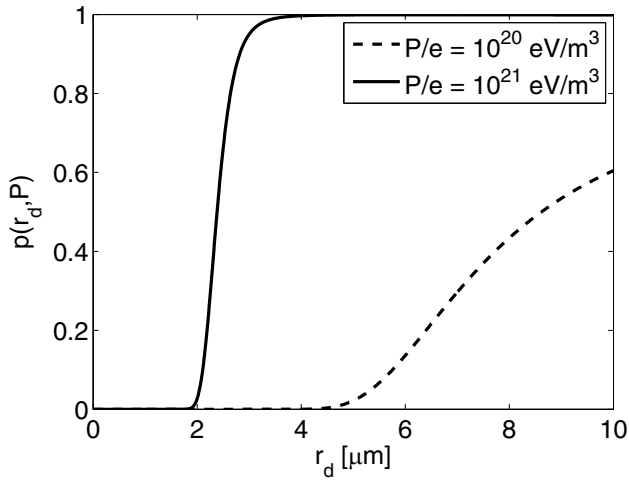
Fig. 3. Remobilization probability against the dust size for various plasma pressures. The surface roughness parameters are taken from Table 1. Results valid as long as $r_d \ll \lambda_D$.

distributed ions is used[47]. To remain consistent with the sheath model from Section 3, a simpler expression derived from monokinetic ions is more suitable. In [3], the Orbital-Motion Limited (OML) cross-section is used, but it is computed for ions flowing in a central force field and makes little sense for a dust particle laying on a planar surface in the presence of an external electric field. To be in line with the sheath model above, the dust projected surface πr_d^2 is preferentially used to approximate its cross-section. This is equivalent to assuming that the electric field is oriented perpendicularly to the surface. Thus the herein presented results hold as long as the dust does not disturb the sheath electric electric field structure, i.e., if it remains small compared to the sheath thickness. In the case of monokinetic ions, the component of the ion drag force perpendicular to the wall, noted F_{id}, is expressed as

$$F_{\mathrm{id}} = \pi r_d^2 m_i n v_{\mathrm{thi}}^2 u_\perp, \tag{10}$$

where $u_\perp = v_i/v_{\mathrm{thi}}$ is the component of the ion velocity perpendicular to the wall. As discussed above, the ion velocity is considered oriented perpendicularly to the wall. In this case, $u_\perp = \sqrt{1 - 2\varphi_w}$. Finally, it is important to note that both F_e and F_{id} depend solely on the plasma pressure at the sheath edge, $P = nT$.

4. Dust remobilization in tokamaks

From Eqs. (1), (2), (6) and (10), the resuspension condition is reached for $F_e > F_a + F_{\mathrm{id}}$. The probability for a dust of given size to be remobilized, noted p, corresponds to the probability for the adhesion force to equal the external force $F_{\mathrm{ex}} = F_e - F_{\mathrm{id}}$. Thus p is given by the cumulative distribution function of adhesion forces evaluated at $F_e - F_{\mathrm{id}}$, i.e.,

$$p(r_d, P) = \frac{1}{2} \mathrm{erfc} \left[-\frac{\log(F_e - F_{\mathrm{id}}) - b}{a\sqrt{2}} \right], \tag{11}$$

where erf is the complementary error function and [29]

$$a = \sqrt{\log \left[\left(\frac{\sigma}{\langle F_a \rangle} \right)^2 + 1 \right]},$$

$$b = \log\langle F_a \rangle + \frac{a^2}{2}. \tag{12}$$

According to our model, this condition varies with the background plasma conditions (pressure P), the dust material (through the Hamaker constant A_H), radius r_d and the surface roughness parameters (rms$_i$ and λ_i). The behavior of the remobilization condition is not straightforward since both the electric and ion drag forces increase in warmer and

denser plasmas and are proportional to r_d^2. The adhesion force is independent of the plasma conditions and varies as $\propto r_d$ for small grains, but quickly saturates for $r_d \gtrsim 1\ \mu m$, as can be seen in Fig. 1. The remobilization probability is plotted in Fig. 3 for W dust laying on a surface with the roughness parameters of the W substrate presented in Table 1.

It can be observed that remobilization occurs preferentially in hot and dense plasmas. Due to the multiple assumptions made and the simplicity of our model, the precise behavior of the curves in Fig. 3 is less important than the following conclusions in steady-state plasmas: (i) dust smaller than $\sim 0.1\ \mu m$ are hardly remobilized; (ii) dust of $\sim 10\ \mu m$ are more easily remobilized. This is in agreement with remobilization experiments performed in [7], where it was observed that metallic grains with $r_d \lesssim 10\ \mu m$ are hardly remobilized in steady-state plasmas with $T \sim 10\ \mathrm{eV}$ and $n \sim 10^{18}\ \mathrm{m}^{-3}$ (thus $P/e \sim 10^{19}\ \mathrm{eV/m}^3$), and that larger grains are more easily remobilized. Indeed, in this case and according to our model, p remains below 1% for $r_d < 10\ \mu m$, then increases up to 20% at $r_d = 20\ \mu m$.

5. Conclusion

Electric fields applied on dust grains deposited onto planar surfaces can lead to remobilization under particular tokamak conditions. The van der Waals-based Rabinovich model for the adhesion force is used since it shows better agreement with mean adhesion force measurements performed with AFM. It is analytically revealed that typical sheath electric fields can lead to micron-size dust remobilization in tokamaks, thereby confirming experimental observations. Simple estimates for the remobilization probability are provided. This effect can cause important impurity seeding in the divertor region of a fusion plasma, especially in the case of a sweeping strike point since the high temperature and high density plasma scans a larger area on the divertor surfaces, thereby impacting a larger amount of dust.

References

[1] S.I. Krasheninnikov, R.D. Smirnov, D.L. Rudakov, Dust in magnetic fusion devices, Plasma Phys. Control. Fusion 53 (8) (2011) 083001.

[2] Y. Tomita, R. Smirnov, T. Takizuka, D. Tskakaya, Charging of a spherical dust particle on a plasma-facing wall, J. Plasma Phys. 72 (6) (2006) 1015–1018, https://doi.org/10.1017/S0022377806005137.

[3] Y. Tomita, R. Smirnov, T. Takizuka, D. Tskhakaya, Gravitational effect on release conditions of dust particle from plasma-facing wall, Contrib. Plasma Phys. 46 (7–9) (2006) 617–622, https://doi.org/10.1002/ctpp.200610053.

[4] R. Smirnov, D. Tskhakaya Y. Tomita, T. Takizuka, Two-dimensional simulation study on charging of dust particle on plasma-facing wall, Contrib. Plasma Phys. 46 (7–9) (2006) 623–627. 10.1002/ctpp.200610054.

[5] Y. Tomita, R. Smirnov, H. Nakamura, S. Zhu, T. Takizuka, D. Tskhakaya, Effect of truncation of electron velocity distribution on release of dust particle from plasma-facing wall, J. Nucl. Mater. 363 (Supplement C) (2007) 264–269, https://doi.org/10.1016/j.jnucmat.2007.01.025. Plasma-Surface Interactions-17

[6] Y. Tomita, R.D. Smirnov, T. Takizuka, D. Tskhakaya, Effect of oblique magnetic field on release conditions of dust particle from plasma-facing wall, Contrib. Plasma Phys. 48 (1–3) (2008) 285–289, https://doi.org/10.1002/ctpp.200810050.

[7] P. Tolias, S. Ratynskaia, M.D. Angeli, G.D. Temmerman, D. Ripamonti, G. Riva, I. Bykov, A. Shalpegin, L. Vignitchouk, F. Brochard, K. Bystrov, S. Bardin, A. Litnovsky, Dust remobilization in fusion plasmas under steady state conditions, Plasma Phys. Control. Fusion 58 (2) (2016) 025009.

[8] K.L. Johnson, K. Kendall, A.D. Roberts, Surface energy and the contact of elastic solids, Proceedings of the Royal Society of London A: Mathematical, Physical and Engineering Sciences 324 (1558) (1971) 301–313, https://doi.org/10.1098/rspa.1971.0141. http://rspa.royalsocietypublishing.org/content/324/1558/301.full.pdf

[9] B. Derjaguin, V. Muller, Y. Toporov, Effect of contact deformations on the adhesion of particles, J. Colloid Interface Sci. 53 (2) (1975) 314–326, https://doi.org/10.1016/0021-9797(75)90018-1.

[10] L. Biasi, A. de los Reyes, M. Reeks, G. de Santi, Use of a simple model for the interpretation of experimental data on particle resuspension in turbulent flows, J. Aerosol Sci. 32 (10) (2001) 1175–1200, https://doi.org/10.1016/S0021-8502(01)00048-9.

[11] N.M. Mokgalapa, T.K. Ghosh, S.K. Loyalka, Graphite particle adhesion to hastelloy x: measurements of the adhesive force with an atomic force microscope, Nucl. Technol. 186 (1) (2014) 45–59, https://doi.org/10.13182/NT13-9.

[12] T. Zhang, W. Peng, K. Shen, S. Yu, AFM Measurements of adhesive forces between carbonaceous particles and the substrates, Nucl. Eng. Des. 293 (2015) 87–96, https://doi.org/10.1016/j.nucengdes.2015.06.022.

[13] H. Krupp, Particle adhesion: theory and experiment, Adv. Colloid Interface Sci. 1 (1967) 111_239.

[14] H. Mizes, M. Ott, E. Eklund, D. Hays, Small particle adhesion: measurement and control, Colloids Surf., A 165 (1–3) (2000) 11–23, https://doi.org/10.1016/S0927-7757(99)00442-2.

[15] G. Salazar-Banda, M. Felicetti, J. Gonçalves, J. Coury, M. Aguiar, Determination of the adhesion force between particles and a flat surface, using the centrifuge technique, Powder Technol. 173 (2) (2007) 107–117, https://doi.org/10.1016/j.powtec.2006.12.011.

[16] P. Petean, M. Aguiar, Determining the adhesion force between particles and rough surfaces, Powder Technol. 274 (2015) 67–76, https://doi.org/10.1016/j.powtec.2014.12.047.

[17] S. Matsusaka, H. Masuda, Particle reentrainment from a fine powder layer in a turbulent air flow, Aerosol Sci. Technol. 24 (2) (1996) 69–84, https://doi.org/10.1080/02786829608965353.

[18] S. Peillon, A. Roynette, C. Grisolia, F. Gensdarmes, Resuspension of carbon dust collected in tore supra and exposed to turbulent airflow: controlled experiments and comparison with model, Fusion Eng. Des. 89 (11) (2014) 2789–2796, https://doi.org/10.1016/j.fusengdes.2014.08.004.

[19] S. Brambilla, S. Speckart, M.J. Brown, Adhesion and aerodynamic forces for the resuspension of non-spherical particles in outdoor environments, J. Aerosol Sci. 112 (2017) 52–67, https://doi.org/10.1016/j.jaerosci.2017.07.006.

[20] S. Ripperger, K. Hein, Measurement of adhesion forces between particles and rough substrates in air with the vibration method, KONA Powder Part. J. 22 (0) (2004) 121–133, https://doi.org/10.14356/kona.2004015.

[21] S. Wanka, M. Kappl, M. Wolkenhauer, H.-J. Butt, Measuring adhesion forces in powder collectives by inertial detachment, Langmuir 29 (52) (2013) 16075–16083, https://doi.org/10.1021/la404014d.

[22] U. Zafar, C. Hare, A. Hassanpour, M. Ghadiri, Drop test: a new method to measure the particle adhesion force, Powder Technol. 264 (2014) 236–241, https://doi.org/10.1016/j.powtec.2014.04.022.

[23] A.Y.H. Cho, Contact charging of micron sized particles in intense electric fields, J. Appl. Phys. 35 (9) (1964) 2561–2564, https://doi.org/10.1063/1.1713799.

[24] D.W. Cooper, H.L. Wolfe, R.J. Miller, Electrostatic Removal of Particles from Surfaces, Particles on Surfaces 1, K. L. Mittal (Ã©d.), New York, 1988, p. 11.

[25] M. Takeuchi, Adhesion forces of charged particles, Chem. Eng. Sci. 61 (7) (2006) 2279–2289, https://doi.org/10.1016/j.ces.2004.06.051.

[26] T.R. Szarek, P.F. Dunn, An apparatus to determine the pull-off force of a conducting microparticle from a charged surface, Aerosol Sci. Technol. 41 (1) (2007) 43–50, https://doi.org/10.1080/02786820601064865.

[27] G. Riva, P. Tolias, S. Ratynskaia, G. Daminelli, R. Donde, M.D. Angeli, E. Vassallo, M. Pedroni, Adhesion measurements for tungsten dust deposited on tungsten surfaces, Nucl. Mater. Energy 12 (2017) 593–598, https://doi.org/10.1016/j.nme.2016.11.009. Proceedings of the 22nd International Conference on Plasma Surface Interactions 2016, 22nd PSI

[28] S. Peillon, M. Sow, C. Grisolia, F. Miserque, F. Gensdarmes, Mobilization of tungsten dust by electric forces and its bearing on tritiated particles in the iter tokamak, J. Electrostat. 88 (Supplement C) (2017) 111–115, https://doi.org/10.1016/j.elstat.2017.01.020. Special Issue on The International Conference on Electrostatics, Electrostatics 2017

[29] P. Tolias, G. Riva, M.D. Angeli, S. Ratynskaia, G. Daminelli, C. Lungu, C. Porosnicu, Adhesive force distributions for tungsten dust deposited on bulk tungsten and beryllium-coated tungsten surfaces, Nucl. Mater. Energy 15 (2018) 55–63, https://doi.org/10.1016/j.nme.2018.05.013.

[30] H. Hamaker, The london van der waals attraction between spherical particles, Physica 4 (10) (1937) 1058–1072, https://doi.org/10.1016/S0031-8914(37)80203-7.

[31] H.-J. Butt, B. Cappella, M. Kappl, Force measurements with the atomic force microscope: technique, interpretation and applications, Surf. Sci. Rep. 59 (1–6) (2005) 1–152, https://doi.org/10.1016/j.surfrep.2005.08.003.

[32] F.L. Leite, C.C. Bueno, A.L. Da Rz, E.C. Ziemath, O.N. Oliveira, Theoretical models for surface forces and adhesion and their measurement using atomic force microscopy, Int. J. Mol. Sci. 13 (12) (2012) 12773–12856, https://doi.org/10.3390/ijms131012773.

[33] Y.I. Rabinovich, J.J. Adler, A. Ata, R.K. Singh, B.M. Moudgil, Adhesion between nanoscale rough surfaces: ii. measurement and comparison with theory, J. Colloid Interface Sci. 232 (1) (2000) 17–24, https://doi.org/10.1006/jcis.2000.7168.

[34] C. Stancu, F. Stokker-Cheregi, A. Moldovan, M. Dinescu, C. Grisolia, G. Dinescu, Modification of w surfaces by exposure to hollow cathode plasmas, Appl. Phys. A 123 (10) (2017) 618, https://doi.org/10.1007/s00339-017-1235-4.

[35] L. Doceul, J. Bucalossi, S. Larroque, M. Lipa, C. Portafaix, A. Saille, F. Samaille, B. Soler, F. Ferlay, J. Verger, Design, integration and feasibility studies of the tore-supra west divertor structure, Fusion Eng. Des. 88 (6) (2013) 814–817, https://doi.org/10.1016/j.fusengdes.2013.01.015. Proceedings of the 27th Symposium On Fusion Technology (SOFT-27); Lige, Belgium, September 24–28, 2012

[36] H. Roche, C. Grisolia, C. Hernandez, X. Courtois, N. Vignal, T. Loarer, C. Pocheau, E. Gauthier, P. Delaporte, L. Mercadier, A. Semerok, D. Farcage, Measurement methods associated to laser ablation technique in layer removal process on plasma facing components, 2009 1st International Conference on Advancements in Nuclear Instrumentation, Measurement Methods and their Applications, (2009), pp. 1–5, https://doi.org/10.1109/ANIMMA.2009.5503749.

[37] E. Gauthier, C. Brosset, H. Roche, E. Tsitrone, B. Pgouri, A. Martinez, P. Languille, X. Courtois, Y. Lallier, M. Salami, Confocal microscopy: a new tool for erosion measurements on large scale plasma facing components in tokamaks, J. Nucl. Mater. 438 (2013) S1216–S1220, https://doi.org/10.1016/j.jnucmat.2013.01.269. Proceedings of the 20th International Conference on Plasma-Surface Interactions in Controlled Fusion Devices

[38] X.-L. Jiang, M. Boulos, Induction plasma spheroidization of tungsten and molybdenum powders, Trans. Nonferr. Metals Soc. Chn. 16 (1) (2006) 13–17, https://doi.org/10.1016/S1003-6326(06)60003-4.

[39] Y. Gan, Invited review article: a review of techniques for attaching micro- and nanoparticles to a probes tip for surface force and near-field optical measurements, Rev. Sci. Instrum. 78 (8) (2007) 081101, https://doi.org/10.1063/1.2754076.

[40] S. Peillon, A. Autricque, F. Gensdarmes, C. Grisolia, O. Pluchery, Adhesion of tungsten microspheres on rough tungsten surfaces using atomic force microscopy, Colloids Surf. A.

[41] P. Tolias, Lifshitz calculations of hamaker constants for fusion relevant materials, Fusion Eng. Des. 133 (2018) 110–116, https://doi.org/10.1016/j.fusengdes.2018.06.002.

[42] J. Israelachvili, Intermolecular and surface forces, Intermolecular and Surface Forces, Elsevier Science, 2015.

[43] T. Jones, T. Jones, Electromechanics of particles, Cambridge University Press, 2005.

[44] M. Sow, R. Widenor, A.R. Akande, K.S. Robinson, R.M. Sankaran, D.J. Lacks, The role of humidity on the lift-off of particles in electric fields, J. Braz. Chem. Soc. 24 (2013) 273–279.

[45] M. Lackowski, A. Jaworek, A. Krupa, Current voltage characteristics of alternating electric field charger, J. Electrostat. 58 (1) (2003) 77–89, https://doi.org/10.1016/S0304-3886(02)00200-0.

[46] Krishnaji, P. Kant, R. Srivastava, Dielectric properties of vacuum-evaporated films of tungsten oxide, Thin Solid Films 30 (2) (1975) 319–323, https://doi.org/10.1016/0040-6090(75)90096-6.

[47] I.H. Hutchinson, Collisionless ion drag force on a spherical grain, Plasma Phys. Control. Fusion 48 (2) (2006) 185.